Hierarchical Visual Feature Aggregation for OCR-Free Document Understanding

Jaeyoo Park [1] **Jin Young Choi**[2] **Jeonghyung Park**[3] **Bohyung Han**[1,2]

[1]ECE & [2]IPAI, Seoul National University
[3]Samsung SDS
`{bellos1203, jychoi999, bhhan}@snu.ac.kr`
`jeong.h.park@samsung.com`

Abstract

We present a novel OCR-free document understanding framework based on pre-trained Multimodal Large Language Models (MLLMs). Our approach employs multi-scale visual features to effectively handle various font sizes within document images. To address the increasing costs of considering the multi-scale visual inputs for MLLMs, we propose the Hierarchical Visual Feature Aggregation (HVFA) module, designed to reduce the number of input tokens to LLMs. Leveraging a feature pyramid with cross-attentive pooling, our approach effectively manages the trade-off between information loss and efficiency without being affected by varying document image sizes. Furthermore, we introduce a novel instruction tuning task, which facilitates the model's text-reading capability by learning to predict the relative positions of input text, eventually minimizing the risk of truncated text caused by the limited capacity of LLMs. Comprehensive experiments validate the effectiveness of our approach, demonstrating superior performance in various document understanding tasks.

1 Introduction

In recent years, significant progress has been made in the development of Multimodal Large Language Models (MLLMs) trained on large-scale datasets [1–5], demonstrating remarkable performance in various tasks, such as visual question answering [6, 7], image captioning [8–10], image-text retrieval [11–13], visual grounding [14, 15] etc. MLLMs also exhibit the emergent capability achieving robust Optical Character Recognition (OCR) [9] performance by leveraging extensive pretraining data. Such advancements highlight the potential of MLLMs for practical and challenging tasks related to document understanding, by reducing reliance on external OCR engines which often struggle with complex layouts and varied fonts. Additionally, OCR-based models typically require additional modules to process explicit OCR outputs, adding to system complexity.

Despite their promising abilities, document understanding frameworks without external OCR engines [16–19] face significant challenges, particularly in considering multiple scales of document images, as text and visual elements often vary in size and style. Complex graphical elements, such as charts and diagrams, along with non-standard layouts, pose additional difficulties for the model due to limited receptive fields. This highlights the need for the frameworks to effectively handle the variability in document scales to achieve accurate and comprehensive understanding.

Our goal is to process visual documents over multiple scales rather than a single fixed scale. However, augmenting visual features for multiple scales inevitably increases costs, which is particularly critical for MLLMs, where LLMs have quadratic complexity due to the self-attention mechanism. To tackle this issue, we propose the Hierarchical Visual Feature Aggregation (HVFA) module to reduce the

38th Conference on Neural Information Processing Systems (NeurIPS 2024).

number of visual tokens by incorporating cross-attentive pooling within a feature pyramid. This design accommodates various document image sizes, effectively balancing the trade-off between information retention and efficiency. By reducing the visual features before feeding them into LLMs, our module maintains the original complexity of the LLMs.

In addition to incorporating multi-scale visual inputs, we introduce novel instruction tuning tasks to ensure the model's comprehensive text reading ability and capture layout information effectively. While [19] proposes reading all of the texts in images, we observed that certain documents contain more texts than LLMs can hold, resulting in information loss during training. To address this challenge, we propose an efficient and effective alternative task of reading, where the model learns to read partial texts in images based on their relative positions. Furthermore, teaching the model to predict the relative positions of given texts, which is an inverse task to the aforementioned reading task, enhances its ability to recognize overall layout information.

The main contributions of our paper are summarized as follows:

- We present a novel framework for OCR-free document understanding, built on a pretrained large-scale multi-modal foundation model, which integrates multi-scale visual features to handle varying font sizes in document images.
- We introduce the Hierarchical Visual Feature Aggregation (HVFA) module, which employs cross-attentive pooling to effectively balance information preservation and computational efficiency, addressing the escalating costs associated with detailed visual inputs.
- We employ a novel instruction tuning task, which aims to predict the relative positions of input text, to enhance the model's comprehensive text reading capability.
- The proposed approach presents remarkable performance gains on the multiple document understanding benchmarks among OCR-free models.

The rest of the paper is organized as follows. Section 2 reviews the related work. The details of our approach are described in Section 3, and the experimental results are presented in Section 4. Finally, we conclude this paper in Section 5.

2 Related Work

This section provides an overview of multimodal large language models and their applications to document understanding tasks. Research on document understanding typically falls into two categories: those that incorporate off-the-shelf OCR engines and those that bypass OCR extractors. From the extensive literature on this topic, we highlight the studies most relevant to our work.

2.1 Multimodal Large Language Models

Contrary to early multimodal learning approaches that focused on joint embedding learning for diverse downstream tasks [1–5, 20–24], recent frameworks [9, 12, 13, 25] have shifted toward generating open-ended language responses by leveraging LLMs [26, 27]. This evolution has contributed to various architectural innovations; GiT [9], BLIP [12], and Qwen-VL [28] pioneer encoder-decoder architectures for unified vision-language understanding and generation. Building upon these foundations, BLIP-2 [13] and mPLUG-Owl [25] introduce resamplers (Q-Formers) to bridge the vision-language modality gap through query-relevant feature extraction and dimensionality reduction. Further advances have come through InstructBLIP [29] and LLaVA [30], which enhance multimodal capabilities by instruction tuning on vision-language conversation data.

Recent studies explore MLLMs' text-reading capabilities and their relationship with image resolution. Wang et al. [9] shows MLLMs gradually learn to read text in images through large-scale pretraining. However, Liu et al. [31] reveals that most MLLMs are constrained by their visual encoder architecture designed only for 224×224 resolution inputs, significantly limiting their ability to capture fine-grained details in text-centric tasks. While Monkey [32] demonstrates enhanced performance by supporting high-resolution inputs, their analysis was limited to single-scale processing. These investigations collectively indicate that, although MLLMs can read text in images, their performance is significantly influenced by input resolutions, affecting their ability to handle diverse font sizes and capture fine-grained textual details.

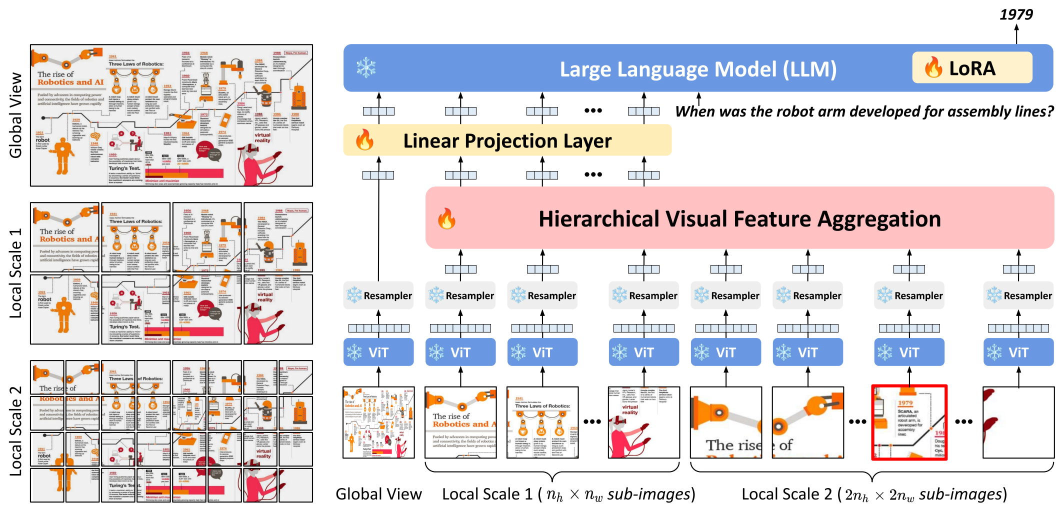
1979
Large Language Model (LLM)
LoRA
When was the robot arm developed for assembly lines?
Linear Projection Layer
Hierarchical Visual Feature Aggregation
Resampler
ViT
Global View
Local Scale 1
Local Scale 2
Local Scale 1 ($n_h \times n_w$ sub-images)
Local Scale 2 ($2n_h \times 2n_w$ sub-images)

Figure 1: Illustration of the proposed framework. Our model adopts visual features from multiple scales, which are aggregated through the Hierarchical Visual Feature Aggregation (HVFA) module. The aggregated features are then fed into an LLM to generate language response in an autoregressive manner. The sub-image highlighted by the red box contains the text relevant to an input question, which requires accurately recognizing visually detailed elements from high resolution image.

2.2 OCR-based Document Understanding Models

Early studies adopted external OCR engines to explicitly model and understand the texts within images [33–39]. LayoutLM [33] directly extends BERT [40] to jointly model interactions between text, visual and layout information for the first time. Based on LayoutLM, there have been efforts to introduce various pretraining objectives to learn layout information effectively by incorporating image-text alignment [34], cell-level information from OCR outputs [36], and multi-modal masking [35, 37]. Despite their strong performance on document understanding benchmarks, these models rely on off-the-shelf OCR engines and struggle with challenging cases such as diverse fonts, handwritten texts, and degraded historical documents. Moreover, they require additional modules for processing OCR results, which increases computational complexity.

2.3 OCR-free Document Understanding Models

To address the drawbacks of OCR-based models, OCR-free models powered by end-to-end multi-modal pretraining have been proposed. Dessurt [16] and Donut [17] combine a learnable visual encoder with an autoregressive text decoder for text recognition. Pix2Struct [18] focuses on layout understanding by learning from HTML data and masked webpage screenshots. However, these methods suffer from high computational costs because they require pretraining models from scratch before task-specific fine-tuning. UReader [19] takes a different approach by leveraging pretrained MLLMs, reducing training costs while handling diverse document types through document instruction tuning and shape-adaptive cropping. Despite these advances, current OCR-free models still struggle to capture diverse visual scales and font sizes, often missing local details in documents.

3 Method

This section describes our main idea, including multi-scale visual inputs, the Hierarchical Visual Feature Aggregation (HVFA) module, and relative text-position prediction tasks in detail.

3.1 Overview

MLLMs generate instruction-following responses given multi-modal inputs, an image I and text (instruction) T. The output token sequence with a length of n_s is denoted by $S = \{s_1, ..., s_{n_s}\}$, where the probability of generating s_i is given by $p(s_i|I, T, S_{<i})$, $1 \leq i \leq n_s$. Given the correct

answer $Y = \{\mathbf{y}_1, ..., \mathbf{y}_{n_y} | \mathbf{y}_i \in \mathbb{R}^{|V|}\}$, where n_y is the length of the answer and V is the vocabulary set, the learning objective of the MLLMs, parameterized by θ, is given by

$$\begin{aligned}\theta^* &= \arg\min_\theta \ \mathcal{L}_{\text{MLLM}}(I, T; \theta) \\ &= \arg\min_\theta \ \frac{1}{|\mathcal{D}|} \sum_{(I,T)\in\mathcal{D}} \left[-\sum_{i=1}^{n_s} \sum_{v=1}^{|V|} \mathbf{y}_{i,v} \log p(s_i = v | I, T, S_{<i}; \theta) \right],\end{aligned} \tag{1}$$

where $\mathcal{D}$ is the image-text dataset.

MLLMs generally comprise three modules: 1) a vision encoder, 2) a projector, and 3) a large language model (LLM). First, we generate visual inputs at multiple scales from a given document image. The vision encoder extracts visual features for detailed image understanding. The resampler-based projector converts these visual features into a compact set of query tokens for the language model. Unlike traditional MLLMs, which feed these query tokens directly into the LLM, we introduce the Hierarchical Visual Feature Aggregation module to reduce the number of visual query tokens while preserving local information. Finally, the LLM processes both the visual and instruction tokens to generate a response autoregressively. Figure 1 illustrates the overall framework.

3.2 Multi-Scale Visual Features

We focus on developing a document understanding framework that incorporates multi-scale visual inputs to address various image scales for MLLMs. However, using pretrained MLLMs constrains the input resolution to a small, square-shaped configuration defined by the visual encoder. This limitation hampers capturing detailed information in high-resolution images and leads to spatial distortions when handling document images of diverse resolutions and aspect ratios.

We adopt shape-adaptive cropping (SAC) [19] to generate multiple sub-images, allowing our model to handle varying aspect ratios and resolutions. We split each image using a predefined grid $\{g = (n_h \times n_w) | n_h, n_w \in \mathbb{N}\}$, where n_h and n_w respectively denote the number of rows and columns for the grid g. Then, each sub-image is resized to fit the visual encoder. Note that the optimal grid $g^* = (n_h^* \times n_w^*)$ for each image is selected by two metrics; resolution coherence, and shape similarity. Refer to Appendix C for more details.

Although SAC handles diverse aspect ratios and high-resolution images, it may miss local details within each sub-image due to its receptive fields of fixed-size. To address this issue, we consider an additional level of detail by applying $2\times$ upscaling to each sub-image to capture detailed visual features and small text fonts through enlarged local resolution. To be specific, this augmentation process involves subdividing each sub-image into half along each spatial dimension, resulting in $2n_h \times 2n_w$ sub-images. We again resize the subdivided images to ensure compatibility with the visual encoder. By incorporating these high-resolution representations, the model now observes the input image in three different levels: global, $n_h \times n_w$, and $2n_h \times 2n_w$ scales.

Unlike vision encoders and resampler-based projectors, which process sub-images in batches and thereby exhibit linear computational complexity, LLMs demonstrate quadratic complexity with respect to the number of sub-images. Thus, when the number of visual inputs increases from n to $5n$, the computational burden of LLMs escalates 25 times, while that of vision encoders and resamplers grows 5 times. Because LLMs are represented by networks with significantly more channels than other models, this quadratic increase of computational cost is problematic in many practice scenarios.

3.3 Hierarchical Visual Feature Aggregation

The HVFA module leverages a feature pyramid to fuse multi-scale features for LLMs and reduces computational overhead. We first construct a feature pyramid using the visual features from two adjacent scales, i^{th} and $(i+1)^{\text{st}}$ scales. Cross-attentive pooling is then applied to features at scale $(i+1)$ to compress and preserve detailed information, and the pooled features are aggregated with low-resolution features at scale i. Figure 2 depicts the mechanism of the HVFA module.

Let $\mathbf{F}_i \in \mathbb{R}^{n_h^i \times n_w^i \times q \times c}$ be the visual features for the i^{th} scale extracted from resampler, where $(n_h^i \times n_w^i)$ is the number of sub-images at i^{th} scale, q denotes the number of queries from resampler, and c is the number of channels. We perform 2×2 max-pooling on $\mathbf{F}_{i+1} \in \mathbb{R}^{n_h^{i+1} \times n_w^{i+1} \times q \times c}$ to

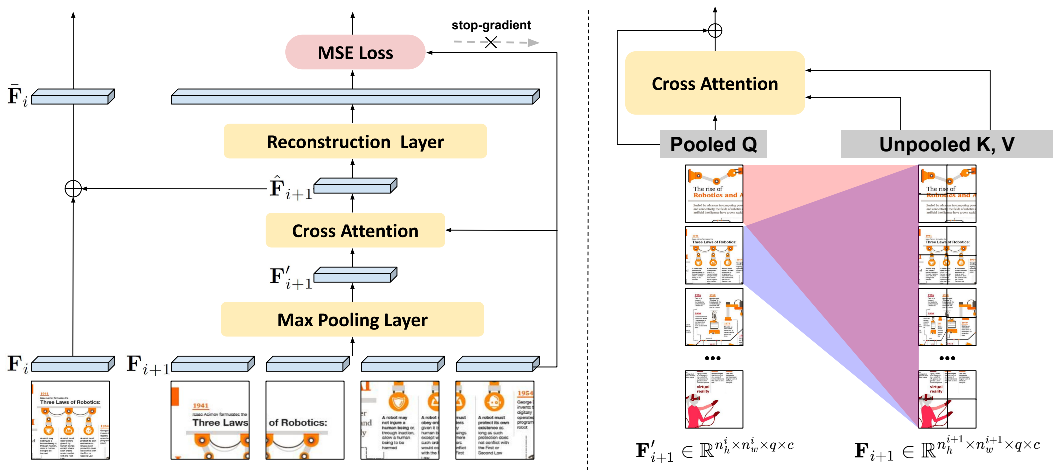

Figure 2: Illustration of the Hierarchical Visual Feature Aggregation (HVFA) module. (Left) HVFA aggregates high-resolution visual features to low-resolution features leveraging feature pyramid structure. (Right) In cross-attentive pooling, each sub-image-feature attends to all of the fine-grained visual features, compressing and preserving more detailed information.

obtain a pooled feature $\mathbf{F}'_{i+1} \in \mathbb{R}^{n_h^i \times n_w^i \times q \times c}$. To reduce the information loss by the max-pooling operation, we conduct the following operations including a lightweight cross-attention:

$$\hat{\mathbf{F}}_{i+1} = \mathbf{F}'_{i+1} + \text{Softmax}\left(\frac{(\mathbf{F}'_{i+1}\mathbf{W}_{\text{query}})(\mathbf{F}_{i+1}\mathbf{W}_{\text{key}})^T}{\sqrt{d}}\right)(\mathbf{F}_{i+1}\mathbf{W}_{\text{value}})\mathbf{W}_{\text{proj}} \tag{2}$$

$$\bar{\mathbf{F}}_i = \mathbf{F}_i + \hat{\mathbf{F}}_{i+1}, \tag{3}$$

where $\mathbf{W}_{\text{query}}, \mathbf{W}_{\text{key}}, \mathbf{W}_{\text{value}} \in \mathbb{R}^{c \times d}$, and $\mathbf{W}_{\text{proj}} \in \mathbb{R}^{d \times c}$are learnable parameters, and d is the embedding dimension. In Equation (3), a pooled feature $\mathbf{F}'_{i+1}$ corresponds to a query and the original feature, $\mathbf{F}_{i+1}$, works as a key and a value. The layer normalization is omitted for simplicity of the expression. We feed $\bar{\mathbf{F}}_i$ to LLMs to generate the language responses. Note that our method maintains the original complexity of LLMs, despite considering multiple scales in practice, because the feature pyramid structure aggregates them into the initial local scale of visual features generated by SAC.

We assume that well-compressed features retain essential information necessary for the reconstruction of the original features. After obtaining the pooled features, based on this assumption, we introduce a small decoder network, used only for training, to reconstruct the original features from the pooled features. The decoder is trained with the mean squared error (MSE) loss between the reconstructed and original features, which is given by

$$\mathcal{L}_{\text{MSE}}(\hat{\mathbf{F}}_{i+1}, \mathbf{F}_{i+1}) = \mathbb{E}[(r(\hat{\mathbf{F}}_{i+1}) - \text{stopgrad}(\mathbf{F}_{i+1}))^2], \tag{4}$$

where $r(\cdot)$ is an MLP-based reconstruction network and stopgrad$(\cdot)$ indicates a stop-gradient operation preventing the collapse in training. By the MSE loss, we guide the model to retain important visual details while reducing feature dimensionality. The final objective function is given by

$$\mathcal{L}_{\text{Final}} = \mathcal{L}_{\text{MLLM}} + \lambda \mathcal{L}_{\text{MSE}}, \tag{5}$$

where λ is the weight for the balance between two terms.

Our approach is similar to pooling-based methods such as MViT [41] and MViT-v2 [42], which construct attention mechanisms utilizing pooled features as keys and values to build efficient ViT variants [43]. However, unlike these methods, we use pooled features as queries to reduce query size rather than optimizing attention mechanisms themselves.

Our cross-attentive pooling can be seen as a form of resampler [13, 44] that reduces spatial dimensionality. In this interpretation, the pooled features, $\mathbf{F}'_{\mathbf{i+1}}$, act as the query tokens for learning. Unlike traditional query-based resamplers that require a new set of trainable query vectors, our method uses pooled features, which are more effective for resampling than randomly initialized query vectors, as discussed further in Section 4.4.

Table 1: Examples for Relative Text-Position Prediction Task. Refer to Appendix I for the full list.

Task	Instruction Templates
RPT (first)	Human: What's in the first 30% of the image text? AI: {corresponding texts}. Human: Identify words from the first 15% of the image text. AI: {corresponding texts}.
RPT (middle)	Human: What are the words located between 10% and 55% of the text in the image? AI: {corresponding texts}. Human: List words found between 20% and 40% in the image text. AI: {corresponding texts}.
RPT (last)	Human: Identify words from the last 16% of the image text. AI: {corresponding texts}. Human: Which words make up the last 40% of the text in the image? AI: {corresponding texts}.
PTP	Human: Specify the relative position within the image where {query texts} is found. AI: 15%-30%. Human: Where is the text {query texts} located within the image? AI: 40%-80%.

3.4 Relative Text-Position Prediction Task

Another key challenge in document understanding is learning to read text using layout information. Although [19] trains models to read entire document text, this approach entails significant computational challenges and information losses due to text truncation caused by the input capacity of LLMs. To address these limitations, we introduce two novel tasks: Reading Partial Text (RPT) and Predicting Text Position (PTP). RPT focuses on reading specific text segments at given positions, while PTP aims to predict the positions of given text segments. These tasks facilitate enhanced layout understanding with reduced computational cost.

Suppose that we can access full document text, represented by a sequence of tokens and we adopt a standard reading order of text (top-to-bottom, left-to-right). For the RPT task, we randomly select one of three types: 1) "*first*": reading up to $p_{end}\%$ of the text, 2) "*middle*": reading from $p_{start}\%$ to $p_{end}\%$ of the text, and 3) "*last*": reading from $p_{start}\%$ to the end. We also sample an instruction template for the selected type, where the instruction template examples are presented in Table 1 and the full list is available in Appendix I. We then compute the maximum text coverage, c_{max}, to mitigate text truncation, which is given by

$$c_{\text{max}} = \min(1.0, l_{\text{max}}/l), \tag{6}$$

where l is the length of the tokenized text and l_{max} is the maximum sequence length acceptable by LLMs.

We set a threshold for the minimum coverage as a hyperparameter, c_{min}, to ensure that sufficient text is read. The range for reading, denoted by t_{range}, is given by

$$t_{\text{range}} = \begin{cases} c_{\text{max}} & \text{if } c_{\text{max}} \le c_{\text{min}} \\ \text{random}(c_{\text{min}}, c_{\text{max}}) & \text{otherwise,} \end{cases} \tag{7}$$

where $\text{random}(a, b)$ denotes a uniform sampling from an interval (a, b). Then, the positions to predict are expressed as follows:

$$(p_{\text{start}}, p_{\text{end}}) = \begin{cases} (0,\ t_{\text{range}}) & \text{if type} = \text{`first'} \\ (p'_{\text{start}},\ p'_{\text{start}} + t_{\text{range}}) & \text{else if type} = \text{`middle'} \\ (100 - t_{\text{range}}, 100) & \text{else if type} = \text{`last'}. \end{cases} \tag{8}$$

where $p'_{start} = \text{random}(0, 100 - t_{\text{range}})$.

For the PTP task, given a segment of text, the model aims to infer its relative position within the whole text. We determine text segments and their relative positions using the same process as in the RPT task. Through diverse training examples, the model learns to understand spatial relationships between text segments and other components in a document.

4 Experiments

4.1 Datasets and Evaluation Metrics

We utilize document instruction dataset corpora for training, following [19]. The training dataset includes various types of document images, including tables, charts, natural images, and web

Table 2: Configurations of OCR-free document understanding baselines.

Method	# Model Params	# Trainable Params	# Pretraining Data	# Fine-tuning data
Document-specific Pretraining				
Dessurt [16]	127M	127M	11M	Task-specific
Donut [17]	143M	143M	13M	Task-specific
Pix2Struct$_{Base}$ [18]	282M	282M	80M	Task-specific
Pix2Struct$_{Large}$ [18]	1.3B	1.3B	80M	Task-specific
MLLM-based Instruction Tuning				
Qwen-VL [28]	9.6B	207M	1.4B+76.8M	Task-specific
Monkey [32]	9.8B	207M	1.4B+76.8M	1.44M
BLIP-2-OPT-2.7B + UReader [19]	3.8B	8M	129M	650K
BLIP-2-OPT-2.7B + Ours	3.8B	14M	129M	650K
mPLUG-Owl-7B + UReader [19]	7.2B	86M	1.1B	650K
mPLUG-Owl-7B + Ours	7.2B	96M	1.1B	650K

Table 3: Performance comparison with other OCR-free document understanding baselines. The bold-faced numbers indicate the best performance in each column.

Method	DocVQA	InfoVQA	DeepForm	KLC	WTQ	TabFact	ChartQA	VisualMRC	TextVQA	TextCaps
Document-specific Pretraining										
Dessurt [16]	63.2	–	–	–	–	–	–	–	–	–
Donut [17]	67.5	11.6	61.6	30.0	18.8	54.6	41.8	93.91	43.5	74.4
Pix2Struct$_{Base}$ [18]	72.1	38.2	–	–	–	–	56.0	–	–	88.0
Pix2Struct$_{Large}$ [18]	76.6	40.0	–	–	–	–	58.6	–	–	95.5
MLLM-based Instruction Tuning										
Qwen-VL [28]	65.1	35.4	4.1	15.9	21.6	–	**65.7**	–	63.8	–
Monkey [32]	66.5	36.1	40.6	32.8	25.3	–	65.1	–	**67.6**	–
BLIP-2-OPT-2.7B + UReader [19]	38.7	22.9	5.6	18.3	17.4	58.5	37.1	214.3	43.2	126.3
BLIP-2-OPT-2.7B + Ours	51.4	29.6	14.6	23.8	21.2	59.9	50.4	**228.7**	57.3	**135.2**
mPLUG-Owl-7B + UReader [19]	65.4	42.2	49.5	32.8	29.4	67.6	59.3	221.7	57.6	118.4
mPLUG-Owl-7B + Ours	**72.7**	**45.9**	**53.0**	**36.7**	**34.5**	**68.2**	63.3	226.4	59.2	123.1

page screenshots. The datasets used are DocVQA [45], InfographicsVQA [46], DeepForm [47], KleisterCharity [48], WikiTableQuestions [49], TabFact [50], ChartQA [51], VisualMRC [52], TextVQA [53], and TextCaps [54]. The combined dataset comprises approximately 650K image-instruction pairs. For more details about the datasets, please refer to Appendix E.

We evaluate our model on the test splits of each dataset. For DocVQA and InfoVQA, we employ the ANLS score [55], while we adopt the F1 score for DeepForm and KLC. The performance on WTQ, TabFact, and TextVQA is measured using accuracy, whereas ChartQA utilizes relaxed accuracy [56]. The metric for TextCaps and VisualMRC is the CIDEr score [57]. Evaluations for TextVQA and TextCaps are conducted on their respective official challenge websites.

4.2 Implementation Details

We conduct experiments on two pretrained resampler-based MLLMs: BLIP-2-OPT-2.7B [13] and mPLUG-Owl-7B [25]. We utilize LoRA [58] to fine-tune the language model efficiently while keeping the vision encoder frozen. For the BLIP-2-based model, we freeze the resampler and apply LoRA, whereas for the mPLUG-Owl-based model, we train the resampler to ensure a fair comparison with [19]. Regarding the SAC, we set the maximum number of sub-images to 9 for the BLIP-2-based model and 20 for the mPLUG-Owl-based model. Refer to Appendix D for more details.

4.3 Quantitative Results

We compare our framework to other OCR-free baselines, including document-specific pretraining approaches [16–18] for completeness. Given that previous methods utilize varying numbers of model parameters, trainable parameters, and training data, we provide the detailed configurations in Table 2. It is important to note that our comparisons are made with OCR-free methods based on comparable MLLMs in terms of model size and dataset scale. Table 3 presents the overall results of the proposed algorithm across 10 document understanding benchmarks. When integrated with both BLIP-2 and mPLUG-Owl, our approach consistently outperforms UReader [19] by a significant margin across all benchmarks. Among MLLM-based methods, our framework outperforms Qwen-

Table 4: Results of main ablation studies with the BLIP-2-based model. Note that the reconstruction loss (Recon) only comes with MS + HVFA.

MS + HVFA	Recon	RTPP	DocVQA	InfoVQA	DeepForm	KLC	WTQ	TabFact	ChartQA	VisualMRC	TextVQA	TextCaps
			35.17	20.34	4.14	18.50	15.36	53.37	31.76	201.39	43.20	126.34
√			45.22	25.87	8.23	19.82	18.14	58.28	44.16	221.38	48.56	129.98
		√	40.18	25.19	6.49	18.97	17.80	56.85	38.88	219.74	47.54	128.39
√	√		47.36	27.37	10.92	19.17	18.24	58.14	46.70	222.56	52.65	130.86
√		√	50.46	28.48	13.18	**23.82**	20.06	59.83	49.48	226.65	56.04	134.06
√	√	√	**51.38**	**29.60**	**14.58**	23.78	**21.15**	**59.87**	**50.41**	**228.65**	**57.32**	**135.24**

Table 5: Ablation study on the variations of hierarchical visual feature aggregation techniques. We employ a BLIP-2-based model for experiments.

Variations	DocVQA	InfoVQA	DeepForm	KLC	WTQ	TabFact	ChartQA	VisualMRC	TextVQA	TextCaps
(a) *Spatial Dimension Reduction*										
Max Pooling-only	43.23	25.44	7.88	19.32	18.14	58.82	44.36	222.49	45.91	126.34
Linear Projectors	46.11	26.44	10.62	21.32	18.74	58.52	46.62	224.74	48.27	129.68
Cross-Attentive Pooling (Ours)	**51.38**	**29.60**	**14.58**	**23.78**	21.15	**59.87**	**50.41**	228.65	**57.32**	**135.24**
Cross-Local-Attentive Pooling	50.32	28.60	14.38	23.56	**22.15**	59.66	50.22	**228.82**	56.78	134.34
(b) *Query Token Initialization*										
Random Vectors	48.07	27.34	11.40	21.82	19.85	58.42	48.01	223.37	53.48	130.22
Max-Pooled Features (Ours)	**51.38**	**29.60**	**14.58**	**23.78**	**21.15**	**59.87**	**50.41**	**228.65**	**57.32**	**135.24**
(c) *Stop-Gradient*										
w/o stopgrad	49.65	26.80	12.16	19.73	19.14	59.11	48.85	223.42	55.24	128.44
w/ stopgrad (Ours)	**51.38**	**29.60**	**14.58**	**23.78**	**21.15**	**59.87**	**50.41**	**228.65**	**57.32**	**135.24**
(d) *Reconstruction Loss*										
$\lambda = 1.0$	49.90	28.51	14.41	22.75	20.13	59.03	49.76	225.51	56.79	133.03
$\lambda = 0.1$ (Ours)	51.38	**29.60**	**14.58**	23.78	**21.15**	**59.87**	**50.41**	**228.65**	**57.32**	**135.24**
$\lambda = 0.01$	**51.84**	28.14	13.84	**23.87**	20.39	59.54	50.05	227.57	57.03	135.17
$\lambda = 0$	50.46	28.48	13.18	23.82	20.06	59.83	49.48	226.65	56.04	134.06

VL-based methods [28, 32] in most benchmarks, despite using a smaller set of pretraining data and smaller model. The results show that our model successfully transfer the knowledge of pretrained MLLMs to understand document samples.

4.4 Ablation Study

We perform several ablation studies with the BLIP-2-based model to validate the effectiveness of each component of our approach.

Effect of each component Based on the results in Table 4, we observe several key findings. First, our multi-scale hierarchical visual feature aggregation (MS + HVFA) significantly improves performance, by leveraging the benefits of multi-scale features. Second, incorporating a reconstruction layer to learn how to reconstruct (Recon) the original features from the pooled features aids in the information compression process, in most cases. Finally, the Relative Text-Position Prediction Task (RTPP) enhances overall performance by improving the model's text-reading ability.

Spatial dimensionality reduction methods Table 5(a) compares different operations for reducing the spatial dimensions of finer-scale features within the HVFA module. Our cross-attentive pooling outperforms simple max-pooling, which suffers from significant information loss due to its non-learnable nature. We also compare our method against a stack of linear projection layers with the same parameter count. The results demonstrate that cross-attentive pooling achieves superior performance by learning more effective feature relationships through its attention mechanism, enabling context-aware information aggregation. Additionally, we investigate a local-attention-based cross-attention mechanism, where the cross-attention is restricted to each sub-image and its corresponding scaled-up features within the feature pyramid. Its slightly inferior results indicate that the pooling operation needs to aggregate information from various regions to be effective.

Query token initialization strategy Our cross-attentive pooling can be regarded as a special form of resampler since it refines high-resolution features while reducing spatial dimensionality. In this

Table 6: Ablation study on text reading tasks. We conduct our ablation study with the BLIP-2-based model. The bold-faced numbers indicate the best performance in each column.

RFT [19]	RPT	PTP	DocVQA	InfoVQA	DeepForm	KLC	WTQ	TabFact	ChartQA	VisualMRC	TextVQA	TextCaps
			47.36	27.37	10.92	19.17	18.24	56.14	43.88	222.56	52.65	130.86
√			49.23	28.16	12.58	21.29	19.42	58.46	46.05	224.39	55.78	133.55
√		√	50.62	29.49	12.55	22.88	20.51	59.28	48.41	226.55	57.19	134.44
	√		50.46	28.44	**14.88**	22.55	20.88	59.12	48.28	226.56	56.91	134.92
	√	√	**51.38**	**29.60**	14.58	**23.78**	**21.15**	**59.87**	**50.41**	**228.65**	**57.32**	**135.14**

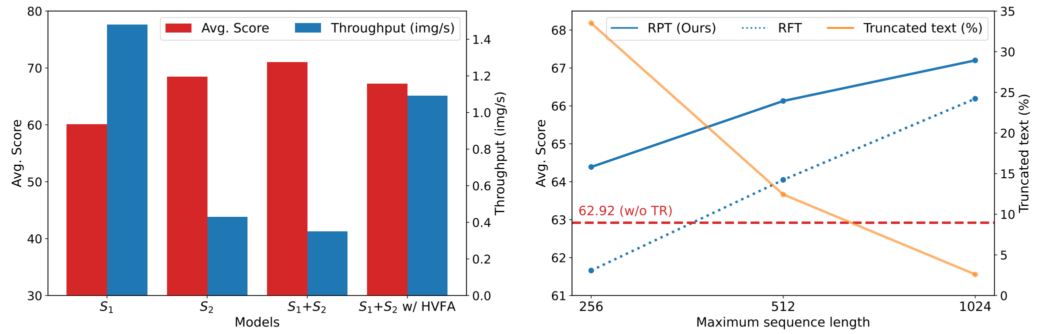

Figure 3: Performance analysis on visual and textual inputs. (Left) Impact of visual input scale on model performance. We compare four variants of our model: with the first scale (S_1), with the second scale (S_2), with multiple scales ($S_1 + S_2$), and with multiple scales with HVFA ($S_1 + S_2$ w/ HVFA, ours). (Right) Impact of truncated text in the text reading task on model performance by varying sequence length capacity of LLM.

context, the pooled features, denoted as $\mathbf{F}'_{i+1}$, serve as query tokens [13, 44] for the learning process. To explore this perspective, we compare our approach with randomly initialized queries of the same size as $\mathbf{F}'_{i+1}$. As demonstrated in Table 5(b), using max-pooled features for query initialization yields superior results, even without tintroducing additional parameters for training.

Role of stop-gradient Table 5(c) presents the role of the "stop-gradient" operation in Equation (4), where the architectures and all hyperparameters remain unchanged. Empirically, $\mathcal{L}_{\text{MSE}}$ drops to zero at an early iteration without the stop-gradient operation due to the convergence at a trivial solution; it leads to a significant degradation in performance.

Impact of λ to balance the loss We tested several different values of λ to determine the optimal balance for the final loss function, $\mathcal{L}_{\text{Final}}$, in Equation (5). Results in Table 5(d) indicate that $\lambda = 0.1$ achieves the best performance. A value of $\lambda = 0.01$ also improves performance compared to $\lambda = 0$, whereas $\lambda = 1.0$ yields worse results than $\lambda = 0$ on some benchmarks. These findings suggest that, while $\mathcal{L}_{\text{MSE}}$ positively contributes by learning compressed features, excessively strong compression hampers the model's primary goal, extracting text-related features.

Effectiveness of relative text-position prediction task Table 6 illustrates the effectiveness of RPT compared to RFT, implying that concentrating on key text segments guided by their relative positions enhances document understanding. Notably, RFT may lead to information loss due to text truncation, given the limited capacity of LLMs. Furthermore, PTP improves the performance of both RPT and RFT tasks, showing that predicting the relative positions of partial text strengthens the model's comprehension of document layout and content. This highlights the importance of considering text position in document understanding tasks.

4.5 Complexity Analysis on Visual Input Scale

To analyze the trade-off between performance and computational cost, we compare variants of our model that process different scales of visual inputs: the first scale (S_1), the second scale (S_2), multiple scales ($S_1 + S_2$), and multiple scales with HVFA ($S_1 + S_2$ w/ HVFA, ours). Figure 3(Left) presents the average benchmark scores and throughput for each model. The throughput is measured on a single NVIDIA Quadro RTX GPU using the largest possible batch size for each model. where the input size

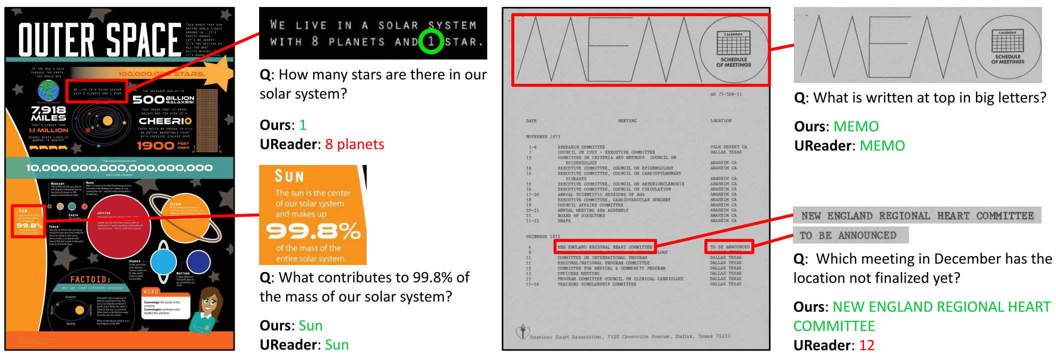
OUTER SPACE
WE LIVE IN A SOLAR SYSTEM WITH 8 PLANETS AND 1 STAR.
SUN
The sun is the center of our solar system and makes up
99.8%
of the mass of the entire solar system.
MEMO
SCHEDULE OF MEETINGS
NEW ENGLAND REGIONAL HEART COMMITTEE
TO BE ANNOUNCED

Q: How many stars are there in our solar system?

Ours: 1
UReader: 8 planets

Q: What contributes to 99.8% of the mass of our solar system?

Ours: Sun
UReader: Sun

Q: What is written at top in big letters?

Ours: MEMO
UReader: MEMO

Q: Which meeting in December has the location not finalized yet?

Ours: NEW ENGLAND REGIONAL HEART COMMITTEE
UReader: 12

Figure 4: Our method vs. UReader [19] on DocVQA [45] and InfographicVQA [46].

of the visual encoder is 224×224. The results indicate that incorporating a finer scale significantly improves performance, albeit with increased computational cost (S_1 vs. S_2). Additionally, combining features from multiple scales boosts performance over single-scale features, though at the expense of higher computational load (S_1, S_2 vs. $S_1 + S_2$). Finally, our method efficiently integrates finer-scale features into a coarser scale, achieving a balance between performance gains and computational demands ($S_1 + S_2$ vs. $S_1 + S_2$ w/ HVFA).

4.6 Analysis on Text Reading Task

To demonstrate the effectiveness and robustness of RPT against truncation, we conducted experiments varying the maximum sequence length of LLMs during training. Figure 3(Right) presents the average benchmark scores and the proportion of truncated text data across the entire dataset. RPT consistently outperforms RFT in all settings, indicating that RPT is robust to the capacity constraints of LLMs. The design of RPT is helpful for mitigating truncation issues while RFT suffers from truncation of text reading data. Notably, with a maximum sequence length of 256, approximately 33.5% of the dataset consists of truncated texts, which is a considerable amount. Consequently, model performance declines even further compared to training without any text-reading task, as represented by the red dotted line in Figure 3(Right). Our approach ensures reliable data quality while incorporating stochasticity and positional information, contributing to its effectiveness. These results imply that our partial text reading task can inspire further research on knowledge distillation and the development of compact models for OCR-related tasks.

4.7 Visualization of Results

Figure 4 illustrates question-answer pairs from the DocVQA [45] and InfographicVQA [46] datasets for comparisons between our framework and UReader [19]. While both models can read large text, our model is more powerful in identifying small text than UReader. This highlights our model's strength in effectively handling text at multiple scales. Furthermore, our method delivers more accurate answers for questions requiring precise reading comprehension. For instance, to answer the question "Which meeting in December has the location not finalized yet?", the model needs to accurately read the text "To be announced" as demonstrated in the rightmost example in Figure 4.

5 Conclusion

We present a novel OCR-free document understanding framework that leverages a pretrained large-scale multi-modal foundation model. Our approach integrates multi-scale visual features to accommodate diverse font sizes within document images. To manage the increasing costs for detailed visual inputs, we propose the Hierarchical Visual Feature Aggregation (HVFA) module with cross-attentive pooling, effectively balancing information retention and computational efficiency while adapting to varying document sizes. Moreover, our framework introduces a novel instruction tuning task to enhance the model's text-reading ability by incorporating positional information within images. Extensive experimentation demonstrates the efficacy of our framework, achieving strong performance across a range of document understanding tasks.

Acknowledgement

This work was partly supported by Samsung SDS, and the Institute of Information & communications Technology Planning & Evaluation (IITP) grants [No.RS-2022-II220959 (No.2022-0-00959), (Part 2) Few-Shot Learning of Causal Inference in Vision and Language for Decision Making, No.RS-2021-II211343, Artificial Intelligence Graduate School Program (Seoul National University), No.RS-2021-II212068, Artificial Intelligence Innovation Hub], and the National Research Foundation of Korea (NRF) grant [No.RS-2022-NR070855, Trustworthy Artificial Intelligence], funded by the Korean government (MSIT).

References

[1] Chen, Y.C., Li, L., Yu, L., El Kholy, A., Ahmed, F., Gan, Z., Cheng, Y., Liu, J.: Uniter: Learning universal image-text representations. In ECCV. (2020)

[2] Kim, W., Son, B., Kim, I.: Vilt: Vision-and-language transformer without convolution or region supervision. In ICML. (2021)

[3] Li, J., Selvaraju, R., Gotmare, A., Joty, S., Xiong, C., Hoi, S.C.H.: Align before fuse: Vision and language representation learning with momentum distillation. In NeurIPS. (2021)

[4] Li, X., Yin, X., Li, C., Zhang, P., Hu, X., Zhang, L., Wang, L., Hu, H., Dong, L., Wei, F., et al.: Oscar: Object-semantics aligned pre-training for vision-language tasks. In ECCV. (2020)

[5] Lu, J., Batra, D., Parikh, D., Lee, S.: Vilbert: Pretraining task-agnostic visiolinguistic representations for vision-and-language tasks. In NeurIPS. (2019)

[6] Suhr, A., Zhou, S., Zhang, A., Zhang, I., Bai, H., Artzi, Y.: A corpus for reasoning about natural language grounded in photographs. In ACL. (2019)

[7] Xie, N., Lai, F., Doran, D., Kadav, A.: Visual entailment: A novel task for fine-grained image understanding. arXiv preprint arXiv:1901.06706 (2019)

[8] Chen, X., Fang, H., Lin, T.Y., Vedantam, R., Gupta, S., Dollár, P., Zitnick, C.L.: Microsoft coco captions: Data collection and evaluation server. arXiv preprint arXiv:1504.00325 (2015)

[9] Wang, J., Yang, Z., Hu, X., Li, L., Lin, K., Gan, Z., Liu, Z., Liu, C., Wang, L.: GIT: A generative image-to-text transformer for vision and language. TMLR (2022)

[10] Yu, J., Wang, Z., Vasudevan, V., Yeung, L., Seyedhosseini, M., Wu, Y.: CoCa: Contrastive captioners are image-text foundation models. TMLR (2022)

[11] Lee, S., Kim, D., Han, B.: Cosmo: Content-style modulation for image retrieval with text feedback. In CVPR. (2021)

[12] Li, J., Li, D., Xiong, C., Hoi, S.: BLIP: Bootstrapping language-image pre-training for unified vision-language understanding and generation. In ICML. (2022)

[13] Li, J., Li, D., Savarese, S., Hoi, S.: BLIP-2: bootstrapping language-image pre-training with frozen image encoders and large language models. In ICML. (2023)

[14] Koh, J.Y., Salakhutdinov, R., Fried, D.: Grounding language models to images for multimodal inputs and outputs. In ICML. (2023)

[15] Yu, L., Poirson, P., Yang, S., Berg, A.C., Berg, T.L.: Modeling context in referring expressions. In ECCV. (2016)

[16] Davis, B., Morse, B., Price, B., Tensmeyer, C., Wigington, C., Morariu, V.: End-to-end document recognition and understanding with dessurt. In ECCV. (2022)

[17] Kim, G., Hong, T., Yim, M., Nam, J., Park, J., Yim, J., Hwang, W., Yun, S., Han, D., Park, S.: Ocr-free document understanding transformer. In ECCV. (2022)

[18] Lee, K., Joshi, M., Turc, I.R., Hu, H., Liu, F., Eisenschlos, J.M., Khandelwal, U., Shaw, P., Chang, M.W., Toutanova, K.: Pix2Struct: Screenshot parsing as pretraining for visual language understanding. In ICML. (2023)

[19] Ye, J., Hu, A., Xu, H., Ye, Q., Yan, M., Xu, G., Li, C., Tian, J., Qian, Q., Zhang, J., et al.: UReader: universal ocr-free visually-situated language understanding with multimodal large language model. In EMNLP. (2023)

[20] Tan, H., Bansal, M.: Lxmert: Learning cross-modality encoder representations from transformers. In EMNLP. (2019)

[21] Gan, Z., Chen, Y.C., Li, L., Zhu, C., Cheng, Y., Liu, J.: Large-scale adversarial training for vision-and-language representation learning. In NeurIPS. (2020)

[22] Zhang, P., Li, X., Hu, X., Yang, J., Zhang, L., Wang, L., Choi, Y., Gao, J.: Vinvl: Revisiting visual representations in vision-language models. In CVPR. (2021)

[23] Huang, Z., Zeng, Z., Huang, Y., Liu, B., Fu, D., Fu, J.: Seeing out of the box: End-to-end pre-training for vision-language representation learning. In CVPR. (2021)

[24] Park, J., Han, B.: Multi-modal representation learning with text-driven soft masks. In CVPR. (2023)

[25] Ye, Q., Xu, H., Xu, G., Ye, J., Yan, M., Zhou, Y., Wang, J., Hu, A., Shi, P., Shi, Y., Jiang, C., Li, C., Xu, Y., Chen, H., Tian, J., Qi, Q., Zhang, J., Huang, F.: mPLUG-Owl: modularization empowers large language models with multimodality. arXiv preprint arXiv:2304.14178 (2023)

[26] Zhang, S., Roller, S., Goyal, N., Artetxe, M., Chen, M., Chen, S., Dewan, C., Diab, M., Li, X., Lin, X.V., et al.: OPT: open pre-trained transformer language models. arXiv preprint arXiv:2205.01068 (2022)

[27] Touvron, H., Lavril, T., Izacard, G., Martinet, X., Lachaux, M.A., Lacroix, T., Rozière, B., Goyal, N., Hambro, E., Azhar, F., et al.: LLaMA: open and efficient foundation language models. arXiv preprint arXiv:2302.13971 (2023)

[28] Bai, J., Bai, S., Yang, S., Wang, S., Tan, S., Wang, P., Lin, J., Zhou, C., Zhou, J.: Qwen-VL: A versatile vision-language model for understanding, localization, text reading, and beyond. arXiv preprint arXiv:2308.12966 (2023)

[29] Dai, W., Li, J., Li, D., Tiong, A.M.H., Zhao, J., Wang, W., Li, B., Fung, P.N., Hoi, S.: Instructblip: Towards general-purpose vision-language models with instruction tuning. In NeurIPS. (2023)

[30] Liu, H., Li, C., Wu, Q., Lee, Y.J.: Visual instruction tuning. In NeurIPS. (2023)

[31] Liu, Y., Li, Z., Li, H., Yu, W., Huang, M., Peng, D., Liu, M., Chen, M., Li, C., Jin, L., et al.: On the hidden mystery of ocr in large multimodal models. arXiv preprint arXiv:2305.07895 (2023)

[32] Li, Z., Yang, B., Liu, Q., Ma, Z., Zhang, S., Yang, J., Sun, Y., Liu, Y., Bai, X.: Monkey: Image resolution and text label are important things for large multi-modal models. arXiv preprint arXiv:2311.06607 (2023)

[33] Xu, Y., Li, M., Cui, L., Huang, S., Wei, F., Zhou, M.: LayoutLM: Pre-training of text and layout for document image understanding. In KDD. (2020)

[34] Xu, Y., Xu, Y., Lv, T., Cui, L., Wei, F., Wang, G., Lu, Y., Florencio, D., Zhang, C., Che, W., et al.: Layoutlmv2: Multi-modal pre-training for visually-rich document understanding. In ACL. (2021)

[35] Huang, Y., Lv, T., Cui, L., Lu, Y., Wei, F.: LayoutLMv3: Pre-training for document ai with unified text and image masking. In ACM. (2022)

[36] Li, C., Bi, B., Yan, M., Wang, W., Huang, S., Huang, F., Si, L.: StructuralLM: Structural pre-training for form understanding. In ACL. (2021)

[37] Appalaraju, S., Jasani, B., Kota, B.U., Xie, Y., Manmatha, R.: DocFormer: End-to-end transformer for document understanding. In ICCV. (2021)

[38] Tang, Z., Yang, Z., Wang, G., Fang, Y., Liu, Y., Zhu, C., Zeng, M., Zhang, C., Bansal, M.: Unifying vision, text, and layout for universal document processing. In CVPR. (2023)

[39] Liao, H., RoyChowdhury, A., Li, W., Bansal, A., Zhang, Y., Tu, Z., Satzoda, R.K., Manmatha, R., Mahadevan, V.: DocTr: Document transformer for structured information extraction in documents. In ICCV. (2023)

[40] Devlin, J., Chang, M.W., Lee, K., Toutanova, K.: Bert: Pre-training of deep bidirectional transformers for language understanding. In NAACL. (2019)

[41] Fan, H., Xiong, B., Mangalam, K., Li, Y., Yan, Z., Malik, J., Feichtenhofer, C.: Multiscale vision transformers. In ICCV. (2021)

[42] Li, Y., Wu, C.Y., Fan, H., Mangalam, K., Xiong, B., Malik, J., Feichtenhofer, C.: Mvitv2: Improved multiscale vision transformers for classification and detection. In CVPR. (2022)

[43] Dosovitskiy, A., Beyer, L., Kolesnikov, A., Weissenborn, D., Zhai, X., Unterthiner, T., Dehghani, M., Minderer, M., Heigold, G., Gelly, S., et al.: An image is worth 16x16 words: Transformers for image recognition at scale. In ICLR. (2021)

[44] Carion, N., Massa, F., Synnaeve, G., Usunier, N., Kirillov, A., Zagoruyko, S.: End-to-end object detection with transformers. In ECCV. (2020)

[45] Mathew, M., Karatzas, D., Jawahar, C.: DocVQA: A dataset for vqa on document images. In WACV. (2021)

[46] Mathew, M., Bagal, V., Tito, R., Karatzas, D., Valveny, E., Jawahar, C.: InfographicVQA. In WACV. (2022)

[47] Svetlichnaya, S.: DeepForm: Understand structured documents at scale (2020)

[48] Stanisławek, T., Graliński, F., Wróblewska, A., Lipiński, D., Kaliska, A., Rosalska, P., Topolski, B., Biecek, P.: Kleister: key information extraction datasets involving long documents with complex layouts. In ICDAR. (2021)

[49] Pasupat, P., Liang, P.: Compositional semantic parsing on semi-structured tables. In ACL. (2015)

[50] Chen, W., Wang, H., Chen, J., Zhang, Y., Wang, H., Li, S., Zhou, X., Wang, W.Y.: TabFact: A large-scale dataset for table-based fact verification. In ICLR. (2020)

[51] Masry, A., Long, D.X., Tan, J.Q., Joty, S., Hoque, E.: ChartQA: A benchmark for question answering about charts with visual and logical reasoning. In ACL. (2022)

[52] Tanaka, R., Nishida, K., Yoshida, S.: VisualMRC: Machine reading comprehension on document images. In AAAI. (2021)

[53] Singh, A., Natarajan, V., Shah, M., Jiang, Y., Chen, X., Batra, D., Parikh, D., Rohrbach, M.: Towards vqa models that can read. In CVPR. (2019)

[54] Sidorov, O., Hu, R., Rohrbach, M., Singh, A.: TextCaps: a dataset for image captioning with reading comprehension. In ECCV. (2020)

[55] Biten, A.F., Tito, R., Mafla, A., Gomez, L., Rusinol, M., Valveny, E., Jawahar, C., Karatzas, D.: Scene text visual question answering. In ICCV. (2019)

[56] Methani, N., Ganguly, P., Khapra, M.M., Kumar, P.: PlotQA: reasoning over scientific plots. In WACV. (2020)

[57] Vedantam, R., Lawrence Zitnick, C., Parikh, D.: CIDEr: consensus-based image description evaluation. In CVPR. (2015)

[58] Hu, E.J., Shen, Y., Wallis, P., Allen-Zhu, Z., Li, Y., Wang, S., Wang, L., Chen, W.: LoRA: Low-rank adaptation of large language models. In ICLR. (2022)

[59] Borchmann, Ł., Pietruszka, M., Stanislawek, T., Jurkiewicz, D., Turski, M., Szyndler, K., Graliński, F.: DUE: End-to-end document understanding benchmark. In NeurIPS Datasets and Benchmarks Track. (2021)

[60] Krasin, I., Duerig, T., Alldrin, N., Ferrari, V., Abu-El-Haija, S., Kuznetsova, A., Rom, H., Uijlings, J., Popov, S., Kamali, S., Malloci, M., Pont-Tuset, J., Veit, A., Belongie, S., Gomes, V., Gupta, A., Sun, C., Chechik, G., Cai, D., Feng, Z., Narayanan, D., Murphy, K.: OpenImages: A public dataset for large-scale multi-label and multi-class image classification. Dataset available from https://storage.googleapis.com/openimages/web/index.html (2017)

[61] Chen, Z., Wang, W., Tian, H., Ye, S., Gao, Z., Cui, E., Tong, W., Hu, K., Luo, J., Ma, Z., et al.: How far are we to gpt-4v? closing the gap to commercial multimodal models with open-source suites. arXiv preprint arXiv:2404.16821 (2024)

[62] Wu, J., Hu, X., Wang, Y., Pang, B., Soricut, R.: Omni-smola: Boosting generalist multimodal models with soft mixture of low-rank experts. In CVPR. (2024)

[63] Chen, X., Wang, X., Beyer, L., Kolesnikov, A., Wu, J., Voigtlaender, P., Mustafa, B., Goodman, S., Alabdulmohsin, I., Padlewski, P., et al.: Pali-3 vision language models: Smaller, faster, stronger. arXiv preprint arXiv:2310.09199 (2023)

[64] Hu, A., Xu, H., Ye, J., Yan, M., Zhang, L., Zhang, B., Li, C., Zhang, J., Jin, Q., Huang, F., et al.: mplug-docowl 1.5: Unified structure learning for ocr-free document understanding. arXiv preprint arXiv:2403.12895 (2024)

[65] Ye, Q., Xu, H., Ye, J., Yan, M., Hu, A., Liu, H., Qian, Q., Zhang, J., Huang, F.: mplug-owl2: Revolutionizing multi-modal large language model with modality collaboration. In CVPR. (2024)

[66] Carbune, V., Mansoor, H., Liu, F., Aralikatte, R., Baechler, G., Chen, J., Sharma, A.: Chart-based reasoning: Transferring capabilities from llms to vlms. arXiv preprint arXiv:2403.12596 (2024)

A Broader Impacts

Research on document understanding and large multimodal language models (MLLMs) can significantly impact various societal domains. In education, they enable personalized learning and greater accessibility to information, while in healthcare, they streamline medical documentation and enhance patient education. Legal and regulatory fields benefit from improved document review and compliance, and businesses gain through advanced customer service and financial analysis tools. However, addressing biases, ensuring privacy, and managing employment impacts are crucial ethical considerations. Moreover, vision system that can understand documents can be used in extracting privacy information from documents easily. Balancing these advancements with societal responsibilities can maximize the benefits for a more informed and equitable society.

B Limitations

Our work has some drawbacks inherited from LLMs, since our work directly employs pretrained LLMs. First, our work is that it is vulnerable to the bias in LLMs, which can cause misinterpreting the crucial and confidential documents. Next, given some document formats, the model may cause the privacy concerns. Our model has been trained only with the documents written in English and thus may struggle the documents written in other languages. While our work employs multi-scale visual features, we still constrains from using resampler-based MLLMs, and thus cannot fully exploit the characteristics of vision encoder, ViT. We believe that our method can directly be adopted to resampler-free pretrained models, since the proposed approach is simple.

C Shape-Adaptive Cropping

Shape-adaptive cropping (SAC) [19] is an image preprocessing method that generates multiple crops to handle varying aspect ratios and resolutions, enhancing versatility and performance. Given an image I with dimensions $H \times W$, we split the image with one of the predefined grids $\{g = (n_h \times n_w) | n_h, n_w \in \mathbb{N}\}$, where n_h, n_w denote the number of rows and columns of the grid g. Each image is then resized to $(n_h H_v, n_w W_v)$ to generate g sub-images, where H_v, and W_v are the spatial configuration defined by the pretrained vision encoder.

The suitable grid $g^* = (n_h^* \times n_w^*)$ for each image is selected based on two criteria; resolution coherence, and shape similarity. It's essential for the grid to maintain the image's resolution to the greatest extent possible, and the grid should conform to the aspect ratio of the input image. Given the predefined set of grids, we denote the resolution-related and resolution-agnostic intersection over union, as s_{rr} and s_{ra}, respectively. s_{rr} and s_{ra} are defined as follows:

$$s_{rr}(I, g) = \text{IoU}((H, W), (n_h H_v, n_w W_v)) \tag{9}$$

$$s_{ra}(I, g) = \text{IoU}((\frac{n_w H}{W}, n_w), (n_h, n_w)). \tag{10}$$

Then the optimal grid g^* is selected by:

$$g^* = \text{argmax}_g (s_{rr}(I, g) + s_{ra}(I, g)). \tag{11}$$

D Implementation Details

We experiment with two pretrained resampler-based MLLMs: BLIP-2-OPT-2.7B [13] and mPLUG-Owl-7B [25]. We utilize LoRA [58] to fine-tune the language model efficiently while keeping the vision encoder frozen. In the case of the resampler, we freeze it and apply LoRA for the BLIP-2-based model, while training it for mPLUG-Owl to ensure a fair comparison to UReader [19]. For LoRA, we set rank $r = 8$, and $\alpha = 32$. The maximum sequence length of the LLM is set to 2048 for all experiments, except for the one described in Section 4.6. Regarding the shape-adaptive cropping module, we set the maximum number of sub-images to 9 for the BLIP-2-based model and 20 for the mPLUG-Owl-based model. We employ the transformers library from huggingface[1] to constuct

[1]`https://huggingface.co/Salesforce/blip2-opt-2.7b`

BLIP-2-based model. For mPLUG-Owl, we implement our algorithm based on the official repository of UReader.[2]

For the Hierarchical Visual Feature Aggregation (HVFA) module, we employed a two-layer multi-head cross-attention layer with $d = 256$ and 12 heads. For $\mathcal{L}_{MSE}$, we utilized a two-layer MLP for the decoder layer and set $\lambda = 0.1$. Regarding the minimum coverage of the Relative Text-Position Prediction Task (RTPP), we set the minimum coverage c_{min} to 30% to ensure that the selected region is not too small.

We trained our model with a learning rate of 1×10^{-4} for 10 epochs, incorporating a linear warmup of 50 steps, followed by cosine decay to 0. The total batch size was set to 256, and we conducted training on 8 A100 GPUs. The entire training time is approximately 2 days for the BLIP-2-based model and 5 days for the mPLUG-Owl-based model.

E Datasets

For all of the benchmarks, we used the train/val/split set provided by UReader [19], which is basically built on DUE benchmark [59].

DocVQA DocVQA [45] consists of 50,000 question and answer (QA) pairs derived from 12,000 document images sourced from the UCSF Industry Documents Library. It comprises 40,000 training questions, 5,000 validation questions, and 5,000 test questions. The evaluation metric utilized is ANLS (Average Normalized Levenshtein Similarity), which measures similarity based on edit distance.

InforgraphicsVQA The InfographicVQA dataset [46] comprises a total of 30,035 questions and 5,485 images sourced from 2,594 distinct web domains. The data is randomly split into 23,946 questions and 4,406 images for training, 2,801 questions and 500 images for validation, and 3,288 questions and 579 images for testing. These questions demand approaches that integrate reasoning across document layout, textual content, graphical elements, and data visualizations simultaneously. We use ANLS for the evaluation metric.

DeepForm DeepForm [47] serves as an information extraction dataset comprising 1100 socially significant documents pertaining to election spending. The objective entails extracting contract numbers, advertiser names, payment amounts, and air dates from advertising disclosure forms submitted to the Federal Communications Commission. The benchmark is evaluated by F1 score.

KleisterCharity KleisterCharity (KLC) [48] represents another information extraction dataset, featuring 2,700 documents sourced from published reports of charity organizations. It tackles significant challenges, including high variability in layout (due to the absence of templates), the necessity of performing Optical Character Recognition (OCR), the presence of lengthy documents, and the existence of various spatial features such as tables, lists, and titles. The evaluation metric utilized is F1 score.

WikiTableQuestions WikiTableQuestions (WTQ) [49] comprises 2.1k table images from Wikipedia and is annotated with 23k question and answer pairs demanding comparison and arithmetic operations. The task necessitates deeper compositionality, leading to a combinatorial explosion within the logical forms space. We use accuracy for the evaluation metric.

TabFact TabFact [50] is a Natural Language Inference dataset comprising 112k statements labeled as 'entailed' or 'refuted' based on information from 16k Wikipedia tables. The dataset is divided into 92,283 statements for training, 12,792 for validation, and 12,779 for testing. The evaluation metric utilized is accuracy.

ChartQA ChartQA [51] is designed to assist users by taking a chart and a natural language question as input to predict the answer. The dataset comprises a total of 21,000 chart images and 32,000 QA pairs, divided into 28,200 for training, 1,920 for validation, and 2,500 for testing. We use relaxed accuracy for the evaluation metric.

[2] `https://github.com/LukeForeverYoung/UReader`.

Table 7: Results of the ablation studies on mPLUG-Owl-based model. Note that the reconstruction loss (Recon) only comes with MS + HVFA.

MS+HVFA	Recon	RFT [19]	RPT	PTP	DocVQA	InfoVQA	DeepForm	KLC	WTQ	TabFact	ChartQA	VisualMRC	TextVQA	TextCaps
√					67.64	43.42	50.34	34.45	27.49	65.75	60.77	211.03	56.47	119.65
√	√				68.14	43.93	50.44	34.58	29.02	66.19	59.25	214.91	56.76	120.55
√			√	√	71.33	45.21	52.42	**36.88**	34.14	68.02	62.90	224.34	58.73	122.32
√	√	√		√	71.77	**45.92**	51.89	36.37	33.71	67.86	62.35	225.60	59.16	122.79
√	√		√	√	**72.68**	45.90	**53.02**	36.73	**34.51**	**68.19**	**63.28**	**226.43**	**59.22**	**123.11**

Table 8: Performance of the BLIP-2-based model with varying scales.

# of scales	Throughput (img/s)	DocVQA	InfoVQA	DeepForm	KLC	WTQ	TabFact	ChartQA	VisualMRC	TextVQA	TextCaps
1	1.481	40.18	25.19	6.49	18.97	17.80	56.85	38.88	219.74	47.54	128.39
2	1.088	51.38	29.60	14.58	23.78	21.15	59.87	50.41	228.65	57.32	135.24
3	0.494	**52.78**	**31.25**	**20.59**	**25.42**	**23.21**	**60.12**	**52.21**	**230.22**	**60.22**	**137.57**

VisualMRC VisualMRC [52] consists of 5,000 full screenshots of webpages from 35 websites, with 30,000 annotated QA pairs. The answers, averaging 9.53 words, are expressed in fluent sentences and are notably longer than those in other QA datasets. The dataset emphasizes natural language understanding and generation, sourcing its questions and abstractive answers from a diverse range of webpage domains. We use CIDEr score for the evaluation metric.

TextVQA TextVQA [53] dataset is designed for evaluating models' abilities to answer questions about images where the answers are textually present within the images. It consists of images from the OpenImagesV3 [60] dataset paired with questions and answers. The dataset comprises approximately 45,336 images, 28,408 training questions, 3,000 validation questions, and 7,684 test questions. We employ accuracy for the evaluation metric.

TextCaps TextCaps [54] dataset is designed for the task of image captioning with a focus on reading and understanding text present in images. It consists of images sourced from the OpenImages dataset, annotated with captions that require the model to recognize and interpret text within the image. The dataset contains over 145,000 images and 230,000 captions. TextCaps challenges models to integrate visual and textual information to generate accurate and informative captions that include text found in the image. We employ the CIDEr score as our evaluation metric.

F Additional Ablation Study Results

To validate the effect of each component more robustly, we conduct the additional ablation study for the mPLUG-Owl-based model. We focused on components that might be considered most marginal: the reconstruction process and Relative Text-Position Prediction (RTPP). Note that we compare RPT to RFT for RTPP experiments. Table 7 shows that the reconstruction loss and RPTT consistently improve performance on most tasks with the large backbone model, mPLUG-Owl.

G Analysis on using more Scales

Our proposed method is inherently flexible, permitting extension to accommodate an arbitrary number of scales. For example, a hierarchical configuration utilizing three scales can be implemented by initially integrating features from scales 3 and 2, followed by merging these with features from scale 1. Table 8 presents the performance across various benchmarks for differing numbers of scales. This experiment employed the BLIP-2-based variant of our model. The findings reveal that the inclusion of a third scale continues to enhance document comprehension, albeit with diminishing returns. This is partly because, as the model has already captured most of the key information from the initial two scales, the additional benefit is reduced. Note that training the model with all three scales without our hierarchical visual feature aggregation module is not feasible on A100 GPUs due to memory constraints.

Table 9: Comparison with task-specific state-of-the-arts methods.

	DocVQA	InfoVQA	DeepForm	KLC	WTQ
SoTA	92.3 (InternVL-1.5-Plus)	75.7 (InternVL-1.5-Plus)	68.8 (mPLUG-DocOwl 1.5)	38.7 (mPLUG-DocOwl 1.5)	40.6 (mPLUG-DocOwl 1.5)
Ours	72.7	45.9	53.0	36.7	34.5

	TabFact	ChartQA	VisualMRC	TextVQA	TextCaps
SoTA	80.4 (mPLUG-DocOwl 1.5)	81.3 (ChartPaLI)	364.2 (LayoutT5)	82.2 (Omni-SMoLA)	164.3 (PaLI-3)
Ours	68.2	63.3	226.4	59.2	123.1

H Comparison with Task-specific SoTA Methods

We list the performance of task-specific state-of-the-art models at the moment of submission in Table 9. The state-of-the-art models can be categorized into 3 categories.

Large Foundation Models These models leverage extensive pretraining datasets and large model parameters. For DocVQA and InfographicsVQA, InternVL-1.5-Plus [61] ranks highest on the leaderboard. This model has 26B parameters and is pretrained on 26 dataset corpora before being fine-tuned on an additional 49 corpora. For TextVQA and TextCaps, variants of PaLI [62, 63] hold the top rank. PaLI, which is trained on the 10B-WebLI dataset, is a significantly stronger foundation model than our backbone, mPLUG-Owl, which only uses a 1B dataset for pretaining. While PaLI-3 [63] has 5B parameters, it still benefits from the 10B-WebLI dataset for pretaining. Moreover, direct comparison becomes more challenging when considering the differences in the unimodal encoders of each model. Note that we have compared our model only with OCR-free methods based on comparable MLLMs in terms of model size and dataset scale.

Methods Using OCR Engines For VisualMRC, current OCR-free models lag behind LayoutT5 [52], which utilizes external OCR engines. This is likely because VisualMRC data is text-rich and features long documents, indicating significant room for improvement. While LayoutT5 has a relatively small model size of 770M parameters compared to recent MLLMs, incorporating OCR engines in such task provides a substantial advantage, particularly in accurately processing and understanding extensive textual information.

Fine-Tuning Foundation Models with Document-Specific Data and Methods Our work falls into this category. For DeepForm, KLC, WTQ, and TabFact, the current SoTA model is mPLUG-DocOwl 1.5 [64], which is a concurrent work to ours. mPLUG-DocOwl 1.5 is based on mPLUG-Owl 2 [65], a direct extension of our backbone, mPLUG-Owl. While the models are similar in size, mPLUG-Owl 2 is known to perform significantly better than mPLUG-Owl. Additionally, mPLUG-DocOwl 1.5 is fine-tuned on 4M document datasets, which is several times more than our 650K dataset. For ChartQA, where ChartPaLI [66] is the state-of-the-arts, instruction data specifically designed for chart data is used, and the model is based on PaLI, pretrained with the 10B-WebLI dataset.

I Instruction Templates for Relative Text-Position Prediction Task

Table 10 illustrates the full list of the templates for Relative Text-Position Prediction Task.

Table 10: Examples for Relative Text-Position Prediction Task

Task	Instruction Templates
RPT (first)	Human: What's in the first { }% of the image text? AI: {corresponding texts}. Human: Identify words from the first { }% of the image text. AI: {corresponding texts}. Human: Which words make up the first { }% of the text in the image? AI: {corresponding texts}. Human: List words in the image text's initial { }% segment. AI: {corresponding texts}. Human: Extract words found in the image text's opening { }%. AI: {corresponding texts}. Human: Words in the initial { }% of the image text? AI: {corresponding texts}. Human: Which words comprise the image text's first { }%? AI: {corresponding texts}. Human: Identify the words positioned in the image text's initial { }%. AI: {corresponding texts}. Human: List the words found within the first { }% of the image text. AI: {corresponding texts}. Human: What words are situated within the initial { }% segment of the image text? AI: {corresponding texts}.
RPT (middle)	Human: What are the words located between { }% and { }% of the text in the image? AI: {corresponding texts}. Human: List words found between { }% and { }% in the image text. AI: {corresponding texts}. Human: Which words fall between { }% and { }% in the image text? AI: {corresponding texts}. Human: What words are in the { }%-{ }% range of the image text? AI: {corresponding texts}. Human: Identify words from { }%-{ }% in the image text? AI: {corresponding texts}. Human: What are the words located at { }%-{ }% in the image text? AI: {corresponding texts}. Human: Can you extract words from { }%-{ }% in the image text? AI: {corresponding texts}. Human: What's within the { }%-{ }% range in the image text? AI: {corresponding texts}. Human: Which words occupy { }%-{ }% of the image text? AI: {corresponding texts}. Human: What words lie between { }% and { }% in the image text? AI: {corresponding texts}.
RPT (last)	Human: Identify words from the last { }% of the image text. AI: {corresponding texts}. Human: Which words make up the last { }% of the text in the image? AI: {corresponding texts}. Human: What's in the last { }% of the image text? AI: {corresponding texts}. Human: List words in the image text's final { }% segment. AI: {corresponding texts}. Human: Extract words found in the image text's closing { }%. AI: {corresponding texts}. Human: Words in the final { }% of the image text? AI: {corresponding texts}. Human: Which words comprise the image text's last { }%? AI: {corresponding texts}. Human: Identify the words positioned in the image text's final { }%. AI: {corresponding texts}. Human: List the words found within the last { }% of the image text. AI: {corresponding texts}. Human: What words are situated within the final { }% segment of the image text? AI: {corresponding texts}.
PTP	Human: Specify the relative position within the image where {query texts} is found. AI: { }%-{ }%. Human: Where is the text {query texts} located within the image? AI: { }%-{ }%. Human: Locate the relative position within the image where the text {query texts} is situated. AI: { }%-{ }%. Human: Determine the relative position within the image where the words {query texts} appear. AI: { }%-{ }%. Human: Identify the relative position within the image where the phrase {query texts} is located. AI: { }%-{ }%. Human: Find the relative position within the image where {query texts} is depicted. AI: { }%-{ }%. Human: Where within the image can we find the phrase {query texts}? AI: { }%-{ }%. Human: At what position in the image do the words {query texts} appear? AI: { }%-{ }%. Human: Where within the image is {query texts} depicted? AI: { }%-{ }%. Human: Where can we locate {query texts} within the image? AI: { }%-{ }%.

NeurIPS Paper Checklist

1. **Claims**

   Question: Do the main claims made in the abstract and introduction accurately reflect the paper's contributions and scope?

   Answer: [Yes]

   Justification: Yes, the main claims made in the abstract and introduction accurately reflect the paper's contributions and scope.

   Guidelines:

   - The answer NA means that the abstract and introduction do not include the claims made in the paper.
   - The abstract and/or introduction should clearly state the claims made, including the contributions made in the paper and important assumptions and limitations. A No or NA answer to this question will not be perceived well by the reviewers.
   - The claims made should match theoretical and experimental results, and reflect how much the results can be expected to generalize to other settings.
   - It is fine to include aspirational goals as motivation as long as it is clear that these goals are not attained by the paper.

2. **Limitations**

   Question: Does the paper discuss the limitations of the work performed by the authors?

   Answer: [Yes]

   Justification: The limitations of our work is stated in the Section B in supplementary file.

   Guidelines:

   - The answer NA means that the paper has no limitation while the answer No means that the paper has limitations, but those are not discussed in the paper.
   - The authors are encouraged to create a separate "Limitations" section in their paper.
   - The paper should point out any strong assumptions and how robust the results are to violations of these assumptions (e.g., independence assumptions, noiseless settings, model well-specification, asymptotic approximations only holding locally). The authors should reflect on how these assumptions might be violated in practice and what the implications would be.
   - The authors should reflect on the scope of the claims made, e.g., if the approach was only tested on a few datasets or with a few runs. In general, empirical results often depend on implicit assumptions, which should be articulated.
   - The authors should reflect on the factors that influence the performance of the approach. For example, a facial recognition algorithm may perform poorly when image resolution is low or images are taken in low lighting. Or a speech-to-text system might not be used reliably to provide closed captions for online lectures because it fails to handle technical jargon.
   - The authors should discuss the computational efficiency of the proposed algorithms and how they scale with dataset size.
   - If applicable, the authors should discuss possible limitations of their approach to address problems of privacy and fairness.
   - While the authors might fear that complete honesty about limitations might be used by reviewers as grounds for rejection, a worse outcome might be that reviewers discover limitations that aren't acknowledged in the paper. The authors should use their best judgment and recognize that individual actions in favor of transparency play an important role in developing norms that preserve the integrity of the community. Reviewers will be specifically instructed to not penalize honesty concerning limitations.

3. **Theory Assumptions and Proofs**

   Question: For each theoretical result, does the paper provide the full set of assumptions and a complete (and correct) proof?

   Answer: [NA]

Justification: We do not have any theoretical results.

Guidelines:

- The answer NA means that the paper does not include theoretical results.
- All the theorems, formulas, and proofs in the paper should be numbered and cross-referenced.
- All assumptions should be clearly stated or referenced in the statement of any theorems.
- The proofs can either appear in the main paper or the supplemental material, but if they appear in the supplemental material, the authors are encouraged to provide a short proof sketch to provide intuition.
- Inversely, any informal proof provided in the core of the paper should be complemented by formal proofs provided in appendix or supplemental material.
- Theorems and Lemmas that the proof relies upon should be properly referenced.

4. **Experimental Result Reproducibility**

   Question: Does the paper fully disclose all the information needed to reproduce the main experimental results of the paper to the extent that it affects the main claims and/or conclusions of the paper (regardless of whether the code and data are provided or not)?

   Answer: [Yes]

   Justification: Implementation details are provided in Section 4.2 in the main paper and Section 4 in the supplementary file.

   Guidelines:

   - The answer NA means that the paper does not include experiments.
   - If the paper includes experiments, a No answer to this question will not be perceived well by the reviewers: Making the paper reproducible is important, regardless of whether the code and data are provided or not.
   - If the contribution is a dataset and/or model, the authors should describe the steps taken to make their results reproducible or verifiable.
   - Depending on the contribution, reproducibility can be accomplished in various ways. For example, if the contribution is a novel architecture, describing the architecture fully might suffice, or if the contribution is a specific model and empirical evaluation, it may be necessary to either make it possible for others to replicate the model with the same dataset, or provide access to the model. In general. releasing code and data is often one good way to accomplish this, but reproducibility can also be provided via detailed instructions for how to replicate the results, access to a hosted model (e.g., in the case of a large language model), releasing of a model checkpoint, or other means that are appropriate to the research performed.
   - While NeurIPS does not require releasing code, the conference does require all submissions to provide some reasonable avenue for reproducibility, which may depend on the nature of the contribution. For example
     (a) If the contribution is primarily a new algorithm, the paper should make it clear how to reproduce that algorithm.
     (b) If the contribution is primarily a new model architecture, the paper should describe the architecture clearly and fully.
     (c) If the contribution is a new model (e.g., a large language model), then there should either be a way to access this model for reproducing the results or a way to reproduce the model (e.g., with an open-source dataset or instructions for how to construct the dataset).
     (d) We recognize that reproducibility may be tricky in some cases, in which case authors are welcome to describe the particular way they provide for reproducibility. In the case of closed-source models, it may be that access to the model is limited in some way (e.g., to registered users), but it should be possible for other researchers to have some path to reproducing or verifying the results.

5. **Open access to data and code**

   Question: Does the paper provide open access to the data and code, with sufficient instructions to faithfully reproduce the main experimental results, as described in supplemental material?

Answer: [NA]

Justification: We used the data UReader [19] provided, which are publicly accessible in `https://github.com/LukeForeverYoung/UReader`.

Guidelines:

- The answer NA means that paper does not include experiments requiring code.
- Please see the NeurIPS code and data submission guidelines (`https://nips.cc/public/guides/CodeSubmissionPolicy`) for more details.
- While we encourage the release of code and data, we understand that this might not be possible, so "No" is an acceptable answer. Papers cannot be rejected simply for not including code, unless this is central to the contribution (e.g., for a new open-source benchmark).
- The instructions should contain the exact command and environment needed to run to reproduce the results. See the NeurIPS code and data submission guidelines (`https://nips.cc/public/guides/CodeSubmissionPolicy`) for more details.
- The authors should provide instructions on data access and preparation, including how to access the raw data, preprocessed data, intermediate data, and generated data, etc.
- The authors should provide scripts to reproduce all experimental results for the new proposed method and baselines. If only a subset of experiments are reproducible, they should state which ones are omitted from the script and why.
- At submission time, to preserve anonymity, the authors should release anonymized versions (if applicable).
- Providing as much information as possible in supplemental material (appended to the paper) is recommended, but including URLs to data and code is permitted.

6. **Experimental Setting/Details**

Question: Does the paper specify all the training and test details (e.g., data splits, hyper-parameters, how they were chosen, type of optimizer, etc.) necessary to understand the results?

Answer: [Yes]

Justification: Implementation details are provided in Section 4.2 in the main paper and Section 4 in the supplementary file.

Guidelines:

- The answer NA means that the paper does not include experiments.
- The experimental setting should be presented in the core of the paper to a level of detail that is necessary to appreciate the results and make sense of them.
- The full details can be provided either with the code, in appendix, or as supplemental material.

7. **Experiment Statistical Significance**

Question: Does the paper report error bars suitably and correctly defined or other appropriate information about the statistical significance of the experiments?

Answer: [No]

Justification: Since our model consists of LLM, which has high computational cost, it is hard to conduct experiment several times.

Guidelines:

- The answer NA means that the paper does not include experiments.
- The authors should answer "Yes" if the results are accompanied by error bars, confidence intervals, or statistical significance tests, at least for the experiments that support the main claims of the paper.
- The factors of variability that the error bars are capturing should be clearly stated (for example, train/test split, initialization, random drawing of some parameter, or overall run with given experimental conditions).
- The method for calculating the error bars should be explained (closed form formula, call to a library function, bootstrap, etc.)

- The assumptions made should be given (e.g., Normally distributed errors).
- It should be clear whether the error bar is the standard deviation or the standard error of the mean.
- It is OK to report 1-sigma error bars, but one should state it. The authors should preferably report a 2-sigma error bar than state that they have a 96% CI, if the hypothesis of Normality of errors is not verified.
- For asymmetric distributions, the authors should be careful not to show in tables or figures symmetric error bars that would yield results that are out of range (e.g. negative error rates).
- If error bars are reported in tables or plots, The authors should explain in the text how they were calculated and reference the corresponding figures or tables in the text.

8. **Experiments Compute Resources**

   Question: For each experiment, does the paper provide sufficient information on the computer resources (type of compute workers, memory, time of execution) needed to reproduce the experiments?

   Answer: [Yes]

   Justification: Implementation details are provided in Section 4.2 in the main paper and Section 4 in the supplementary file.

   Guidelines:

   - The answer NA means that the paper does not include experiments.
   - The paper should indicate the type of compute workers CPU or GPU, internal cluster, or cloud provider, including relevant memory and storage.
   - The paper should provide the amount of compute required for each of the individual experimental runs as well as estimate the total compute.
   - The paper should disclose whether the full research project required more compute than the experiments reported in the paper (e.g., preliminary or failed experiments that didn't make it into the paper).

9. **Code Of Ethics**

   Question: Does the research conducted in the paper conform, in every respect, with the NeurIPS Code of Ethics `https://neurips.cc/public/EthicsGuidelines`?

   Answer: [Yes]

   Justification: We do not have any violation to the code of ethics.

   Guidelines:

   - The answer NA means that the authors have not reviewed the NeurIPS Code of Ethics.
   - If the authors answer No, they should explain the special circumstances that require a deviation from the Code of Ethics.
   - The authors should make sure to preserve anonymity (e.g., if there is a special consideration due to laws or regulations in their jurisdiction).

10. **Broader Impacts**

    Question: Does the paper discuss both potential positive societal impacts and negative societal impacts of the work performed?

    Answer: [Yes]

    Justification: We provide the broader impacts of our work in section 1 in the supplementary file.

    Guidelines:

    - The answer NA means that there is no societal impact of the work performed.
    - If the authors answer NA or No, they should explain why their work has no societal impact or why the paper does not address societal impact.
    - Examples of negative societal impacts include potential malicious or unintended uses (e.g., disinformation, generating fake profiles, surveillance), fairness considerations (e.g., deployment of technologies that could make decisions that unfairly impact specific groups), privacy considerations, and security considerations.

- The conference expects that many papers will be foundational research and not tied to particular applications, let alone deployments. However, if there is a direct path to any negative applications, the authors should point it out. For example, it is legitimate to point out that an improvement in the quality of generative models could be used to generate deepfakes for disinformation. On the other hand, it is not needed to point out that a generic algorithm for optimizing neural networks could enable people to train models that generate Deepfakes faster.
- The authors should consider possible harms that could arise when the technology is being used as intended and functioning correctly, harms that could arise when the technology is being used as intended but gives incorrect results, and harms following from (intentional or unintentional) misuse of the technology.
- If there are negative societal impacts, the authors could also discuss possible mitigation strategies (e.g., gated release of models, providing defenses in addition to attacks, mechanisms for monitoring misuse, mechanisms to monitor how a system learns from feedback over time, improving the efficiency and accessibility of ML).

11. **Safeguards**

    Question: Does the paper describe safeguards that have been put in place for responsible release of data or models that have a high risk for misuse (e.g., pretrained language models, image generators, or scraped datasets)?

    Answer: [NA]

    Justification: Since we do not release our model, we do not have risk for misuse.

    Guidelines:

    - The answer NA means that the paper poses no such risks.
    - Released models that have a high risk for misuse or dual-use should be released with necessary safeguards to allow for controlled use of the model, for example by requiring that users adhere to usage guidelines or restrictions to access the model or implementing safety filters.
    - Datasets that have been scraped from the Internet could pose safety risks. The authors should describe how they avoided releasing unsafe images.
    - We recognize that providing effective safeguards is challenging, and many papers do not require this, but we encourage authors to take this into account and make a best faith effort.

12. **Licenses for existing assets**

    Question: Are the creators or original owners of assets (e.g., code, data, models), used in the paper, properly credited and are the license and terms of use explicitly mentioned and properly respected?

    Answer: [Yes]

    Justification: We properly cited the original papers for all datasets and codebases we used.

    Guidelines:

    - The answer NA means that the paper does not use existing assets.
    - The authors should cite the original paper that produced the code package or dataset.
    - The authors should state which version of the asset is used and, if possible, include a URL.
    - The name of the license (e.g., CC-BY 4.0) should be included for each asset.
    - For scraped data from a particular source (e.g., website), the copyright and terms of service of that source should be provided.
    - If assets are released, the license, copyright information, and terms of use in the package should be provided. For popular datasets, `paperswithcode.com/datasets` has curated licenses for some datasets. Their licensing guide can help determine the license of a dataset.
    - For existing datasets that are re-packaged, both the original license and the license of the derived asset (if it has changed) should be provided.

- If this information is not available online, the authors are encouraged to reach out to the asset's creators.

13. **New Assets**

    Question: Are new assets introduced in the paper well documented and is the documentation provided alongside the assets?

    Answer: [NA]

    Justification: We do not release any new assets for this submission.

    Guidelines:

    - The answer NA means that the paper does not release new assets.
    - Researchers should communicate the details of the dataset/code/model as part of their submissions via structured templates. This includes details about training, license, limitations, etc.
    - The paper should discuss whether and how consent was obtained from people whose asset is used.
    - At submission time, remember to anonymize your assets (if applicable). You can either create an anonymized URL or include an anonymized zip file.

14. **Crowdsourcing and Research with Human Subjects**

    Question: For crowdsourcing experiments and research with human subjects, does the paper include the full text of instructions given to participants and screenshots, if applicable, as well as details about compensation (if any)?

    Answer: [NA]

    Justification: The paper does not involve crowdsourcing nor research with human subjects.

    Guidelines:

    - The answer NA means that the paper does not involve crowdsourcing nor research with human subjects.
    - Including this information in the supplemental material is fine, but if the main contribution of the paper involves human subjects, then as much detail as possible should be included in the main paper.
    - According to the NeurIPS Code of Ethics, workers involved in data collection, curation, or other labor should be paid at least the minimum wage in the country of the data collector.

15. **Institutional Review Board (IRB) Approvals or Equivalent for Research with Human Subjects**

    Question: Does the paper describe potential risks incurred by study participants, whether such risks were disclosed to the subjects, and whether Institutional Review Board (IRB) approvals (or an equivalent approval/review based on the requirements of your country or institution) were obtained?

    Answer: [NA]

    Justification: We do not have any experiments on human subjects nor crowdsourcing.

    Guidelines:

    - The answer NA means that the paper does not involve crowdsourcing nor research with human subjects.
    - Depending on the country in which research is conducted, IRB approval (or equivalent) may be required for any human subjects research. If you obtained IRB approval, you should clearly state this in the paper.
    - We recognize that the procedures for this may vary significantly between institutions and locations, and we expect authors to adhere to the NeurIPS Code of Ethics and the guidelines for their institution.
    - For initial submissions, do not include any information that would break anonymity (if applicable), such as the institution conducting the review.